

Supporting Information

A Dual-Emitting 4d-4f Nanocrystalline Metal-Organic Framework as a Self-Calibrating Luminescent Sensor for Indoor Formaldehyde Pollution

Ji-Na Hao and Bing Yan*

Shanghai Key Lab of Chemical Assessment and Sustainability, Department of Chemistry, Tongji University, Siping Road 1239, Shanghai 200092, China.

Experimental details

Materials and Methods. The salts of $\text{Eu}(\text{NO}_3)_3 \cdot 6\text{H}_2\text{O}$ were prepared by dissolving the corresponding oxide compounds in excess nitric acid followed by evaporation and crystallization. Zirconium tetrachloride and pyromellitic acid was purchased from Adamas and used directly without further purification. All the other starting materials and reagents were all AR and used as purchased. Powder X-ray diffraction (XRD) patterns were obtained on a Bruker D8 Focus diffractometer with Cu K α radiation ($\lambda = 1.5418 \text{ \AA}$, continuous, 40 kV, 40 mA, increment = 0.02°). The gas adsorption/desorption isotherms for N_2 at 77 K were performed on a Tristar 3000 analyzer. Transmission electron microscopy (TEM) was carried out using a JEOL JEM-2100F electron microscope and operated at 200 kV. X-ray photoelectron spectroscopy (XPS) experiments were carried out on a RBD upgraded PHI-5000C ESCA system (Perkin Elmer) with MgK α radiation ($h\nu = 1253.6 \text{ eV}$). Inductively coupled plasma-mass spectrometry (ICP-MS) data were collected on an X-7 series inductively coupled plasma-mass spectrometer (Thermo Elemental, Cheshire, UK). The Fourier transform infrared (FT-IR) spectra were recorded on a Nexus 912 A0446 infrared spectrum spectrophotometer with KBr pellets within the 4000 – 400 cm^{-1} region. The fluorescence spectra were measured on an Edinburgh FLS920 fluorescence spectrophotometer, equipped with a 450 W Xe lamp as the excitation source. The absolute external luminescent quantum efficiency was determined employing an integrating sphere (150 mm diameter, BaSO_4 coating) from an Edinburgh FLS920 phosphorimeter.

Preparation of $\text{Uio-66}(\text{Zr})-(\text{COOH})_2$ (1). To synthesize the title compound, a mixture of 1,2,4,5-benzenetetracarboxylic acid (H_4btcc , 4.3 g, 0.017 mol), Zirconium tetrachloride (ZrCl_4 , 2.3 g, 0.01 mol), and distilled water (50 mL) were placed in a round-bottom flask equipped with a reflux condenser and a magnetic stirrer. This mixture was refluxed (100°C) under air for 24 h resulting in white gel, which was separated by centrifugation and washed thoroughly several times with distilled water. To remove the organic species encapsulated within the pores as much as possible, the activation was further carried out by dispersing the sample in the distilled water ($\sim 10 \text{ mL}$ per 1g of product) and heated under reflux for 16 h. The solid was then recovered by centrifugal separation, washed with acetone and dried at 30°C under vacuum, yielding $\sim 5.0 \text{ g}$ of white powder.

Synthesis of $\text{Ag}^+/\text{Eu}^{3+}$ -1 (1a–1e). Luminescent heterometallic co-doped MOFs were prepared by introducing the silver ions and europium ions into the pores of compound 1. 100 mg of the as-prepared 1 were soaked in 20 mL of distilled water containing $\text{Eu}(\text{NO}_3)_3 \cdot 6\text{H}_2\text{O}$ (0.05 mmol) and different amounts of AgNO_3 (0, 1, 2, 3, 4 mmol). After one day soakage under stirring and dark condition, the solid was then collected by centrifugation, extensively washed with water, and dried at 30°C under vacuum. For convenience, the as-obtained samples with different Ag^+ doping (0, 1, 2, 3, and 4 mmol) are named as 1a, 1b, 1c, 1d and 1e.

Fabrication of luminescent films. The 1a–1e films were prepared by spin-coating method through dropping the alcoholic suspensions of 1a–1e onto the pre-cleaned substrate which was fixed on a Laurell spin-coater. The spin-coating speed and time was kept at 1500 rpm for 30 s. The spin-coating process was repeated several times, and then the film was dried at room temperature.

Vapor sensing. The fabricated luminescent films were used for vapor sensing experiments. For each experiment, the luminescent spectra of the films were measured before exposure to various solvent vapors. The film was then carefully placed into a sealed container ($\sim 20 \text{ mL}$ glass bottle) which contains $\sim 5 \text{ mL}$ of a given solvent for 1h at 25°C , as shown below. Subsequently the film was taken out of the container, and its emission spectrum was quickly taken again.

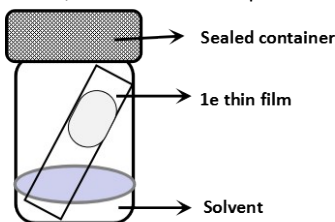


Diagram of gas-sensing measurements for solvent vapors

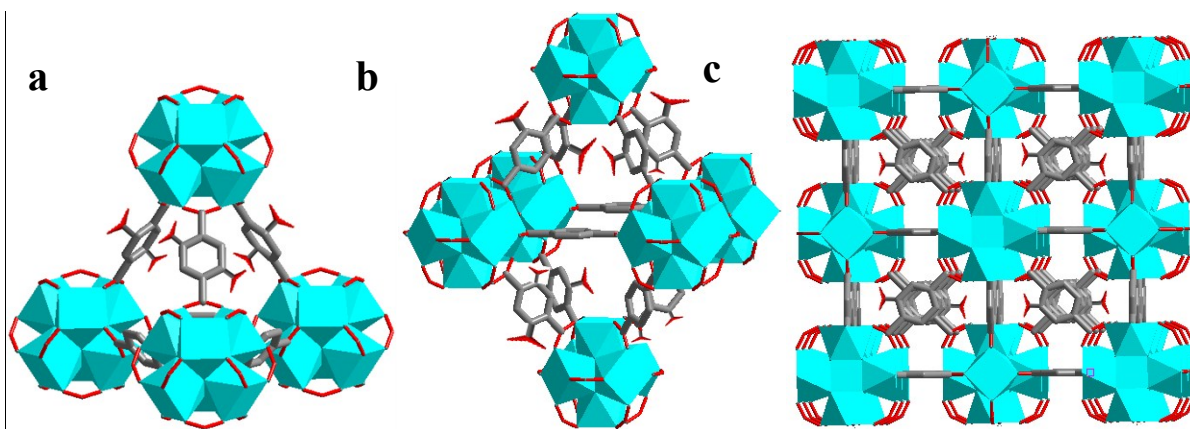


Figure S1. Structure of **1**: (a) tetrahedral cage; (b) octahedral cage; and (c) packing of the two types of cages.

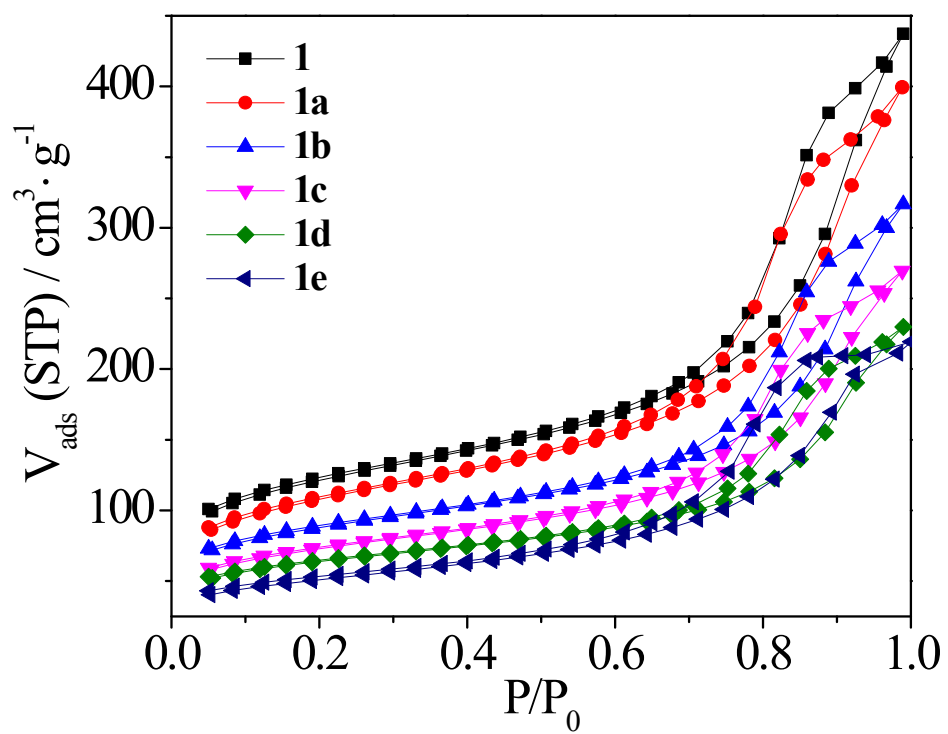


Figure S2. N_2 adsorption-desorption isotherms of **1–1e** samples.

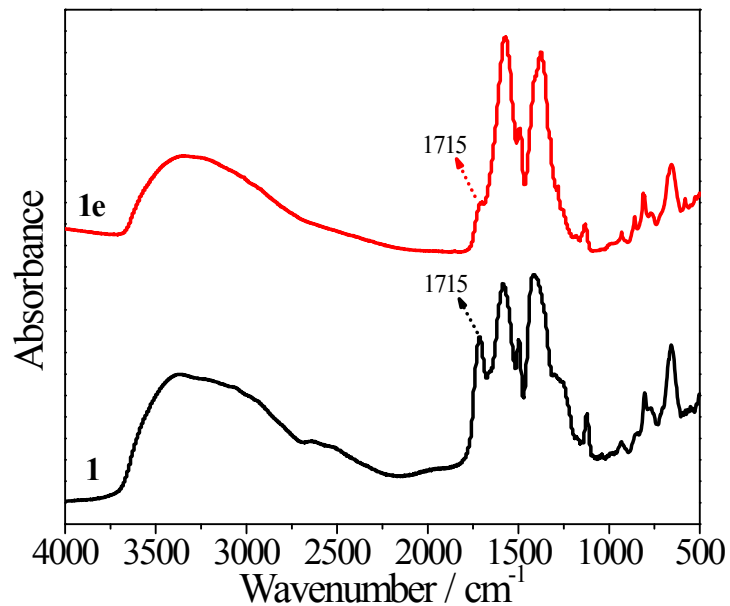


Figure S3. FT-IR spectra of compound **1** and **1e**.

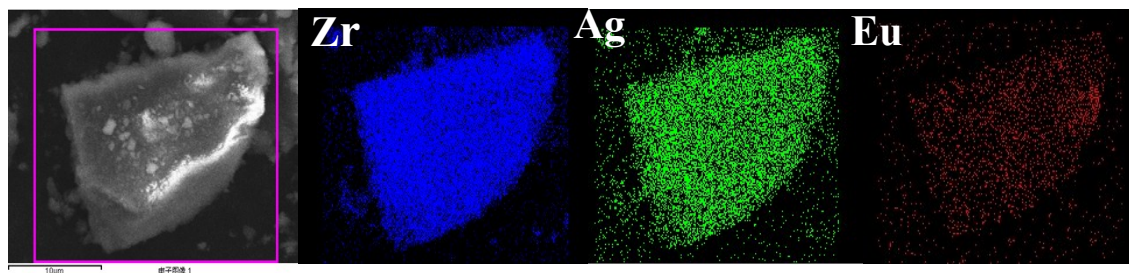


Figure S4. EDX mappings of the Zr, Ag, and Eu elements in **1e**.

Table S1. The detailed ICP-MS studies of **1a–1e** samples.

Materials	Zr ⁴⁺	Eu ³⁺	Ag ⁺	Zr ⁴⁺	Eu ³⁺	Ag ⁺	Zr : Eu : Ag
	(ppm)	(ppm)	(ppm)	(mM)	(mM)	(mM)	
1a	9.852	2.751	0	0.108	0.0181	0	5.97:1:0
1b	7.480	2.067	2.654	0.082	0.0136	0.0246	6.03:1:1.81
1c	12.04	3.343	6.451	0.132	0.022	0.0598	6.00:1:2.72
1d	12.86	3.602	8.565	0.141	0.0237	0.0794	5.95:1:3.35
1e	8.119	2.264	7.357	0.089	0.0149	0.0682	5.97:1:4.58

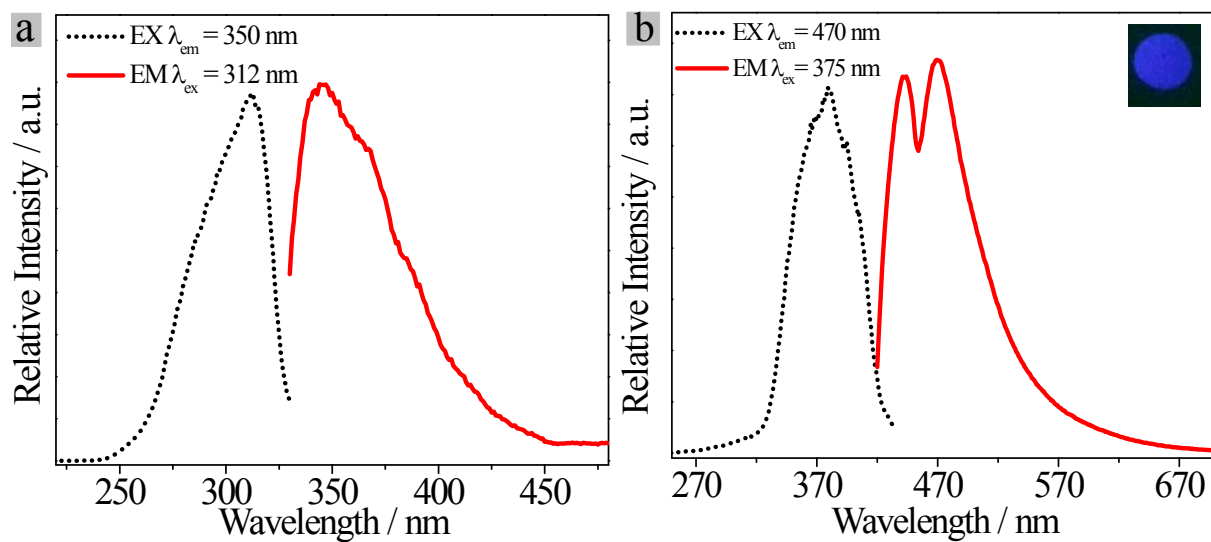


Figure S5. The excitation (black line) and emission (red line) spectra of H₄btcc (a) and compound **1** (b). The inset in (b) shows the corresponding photograph under 365 nm UV-light irradiation.

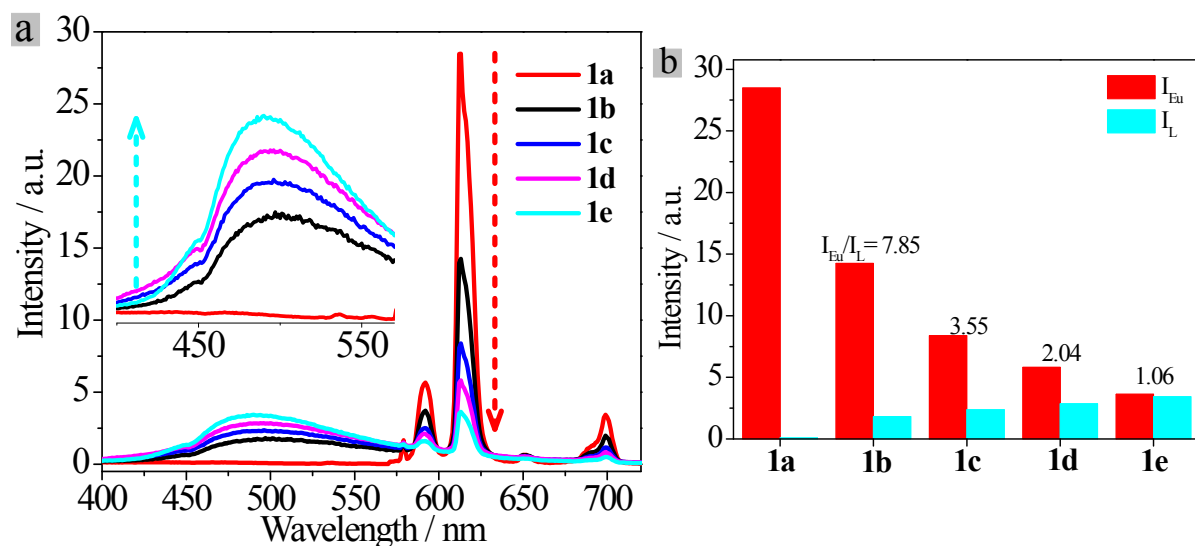


Figure S6. (a) The emission spectra of **1a-1e** (λ_{ex} = 330 nm), inset shows the enlarged spectra of **1a-1e** in the range of 400-570 nm; (b) the luminescence intensities of Eu³⁺ at 613 nm (red bar) and the ligand at 490 nm (cyan bar) in **1a-1e**.

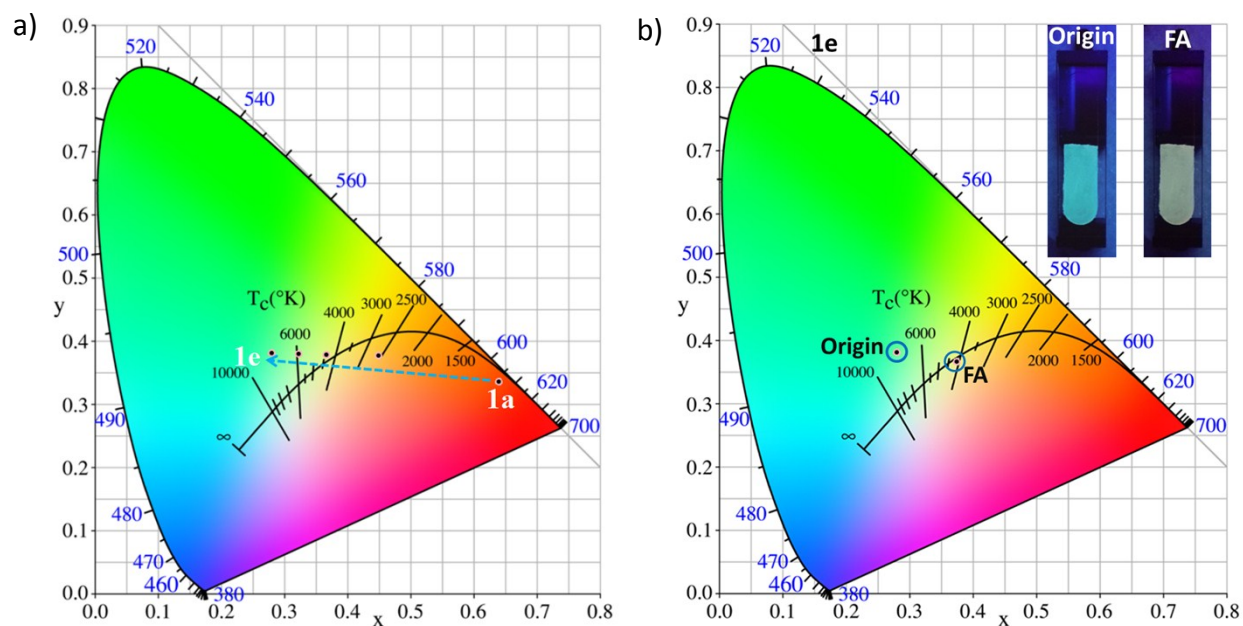


Figure S7. a) The CIE chromaticity coordinates of **1a–1e** calculated from the emission spectra shown in Figure S6a, which shows the luminescent color changes with the increase of Ag⁺-doping; b) The CIE chromaticity coordinates and the photographs of **1e** before and after treated by FA.

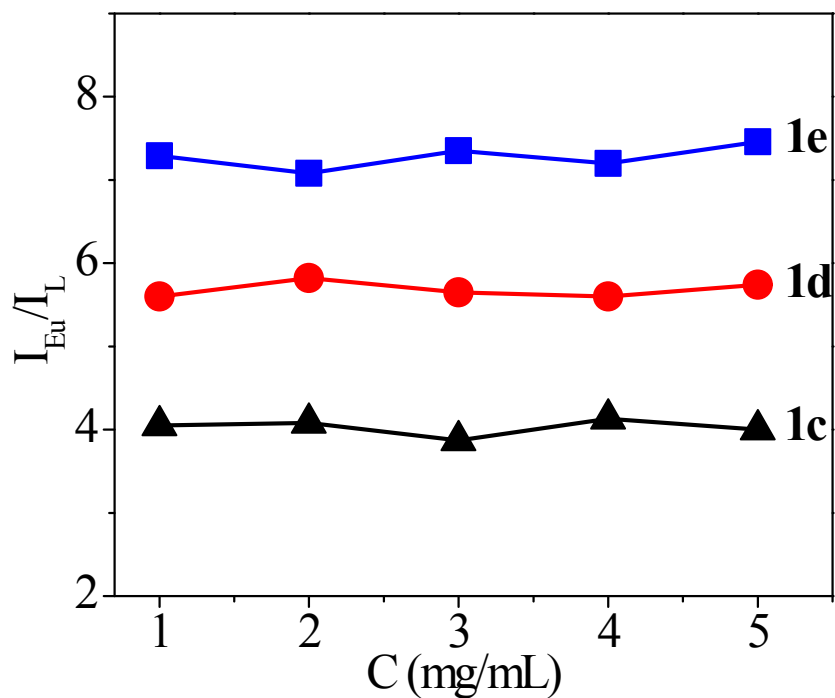


Figure S8. The intensity ratios (I_{Eu}/I_L) of FA treated **1c–1e** films fabricated by different concentrations of **1c–1e** ethanol suspensions.

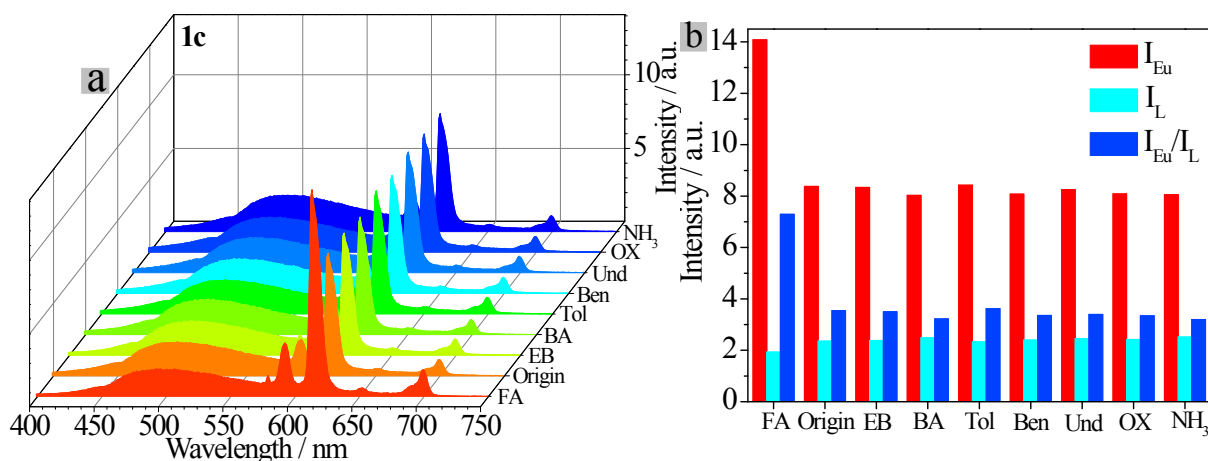


Figure S9. The luminescence spectra (a) and the intensities (I_{Eu} , I_L and I_{Eu}/I_L) (b) of **1c** films after treated by various indoor polluted gases.

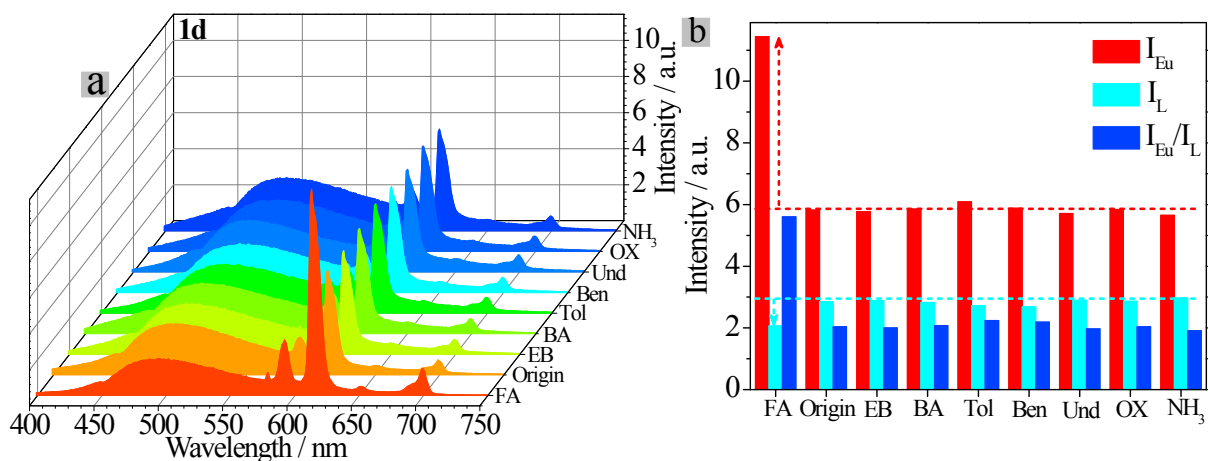


Figure S10. The emission spectra (a) and the intensities (I_{Eu} , I_L and I_{Eu}/I_L) (b) of **1d** films after treated by various indoor polluted gases.

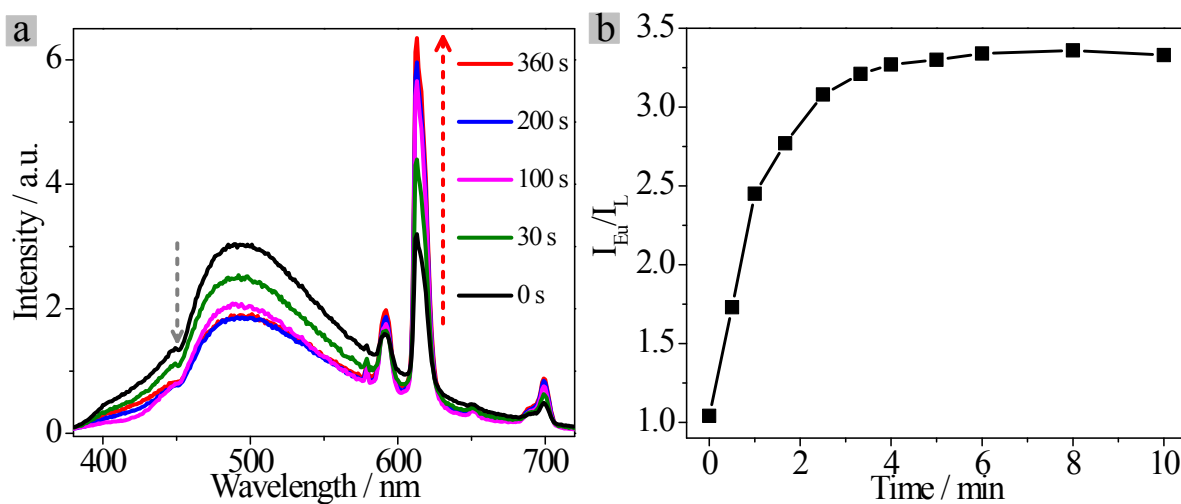


Figure S11. (a) The emission spectra of the **1e** film upon exposed to FA gas at various time intervals ($\lambda_{ex} = 330$ nm) and (b) the intensity (I_{Eu}/I_L) as a function of exposure time.

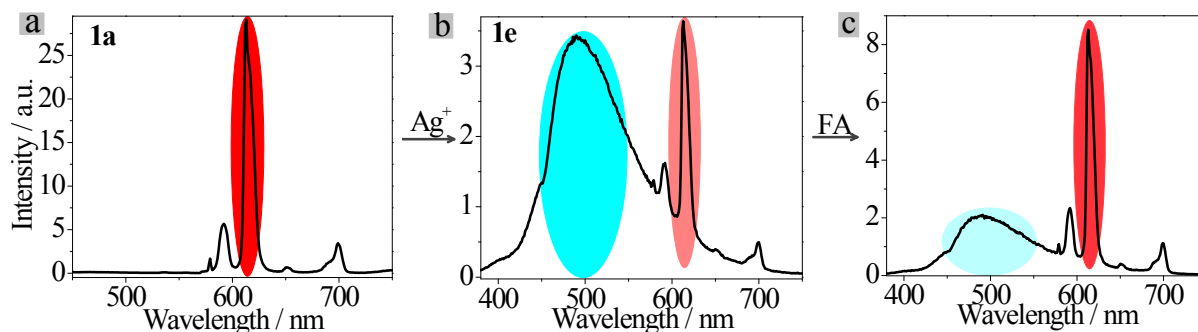


Figure S12. The emission spectra of **1a**, **1e** and FA treated **1e**.

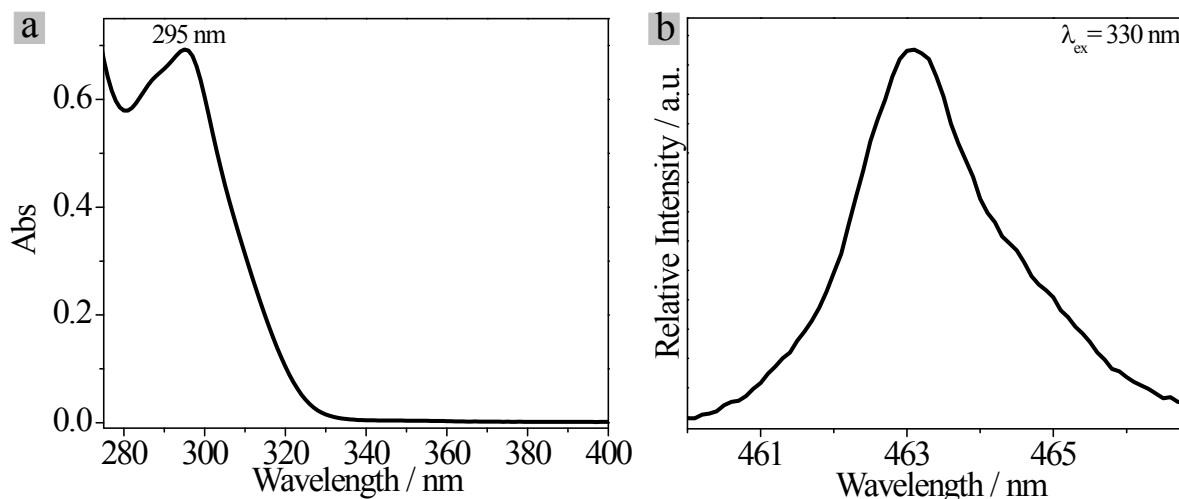


Figure S13. (a) UV-vis absorption spectrum of the ligand in **1e** and (b) the phosphorescence spectrum of $\text{Ag}^+/\text{Gd}^{3+}$ -**1** analogous to **1e** at 77 K. Because the ${}^6\text{P}_{7/2} - {}^8\text{S}_{7/2}$ Gd^{3+} transition occurs at high energy (ca. 32000 cm^{-1}), which presents the ligand-to-metal energy transfer, the observed peak is ascribed to a triplet ligand emission.

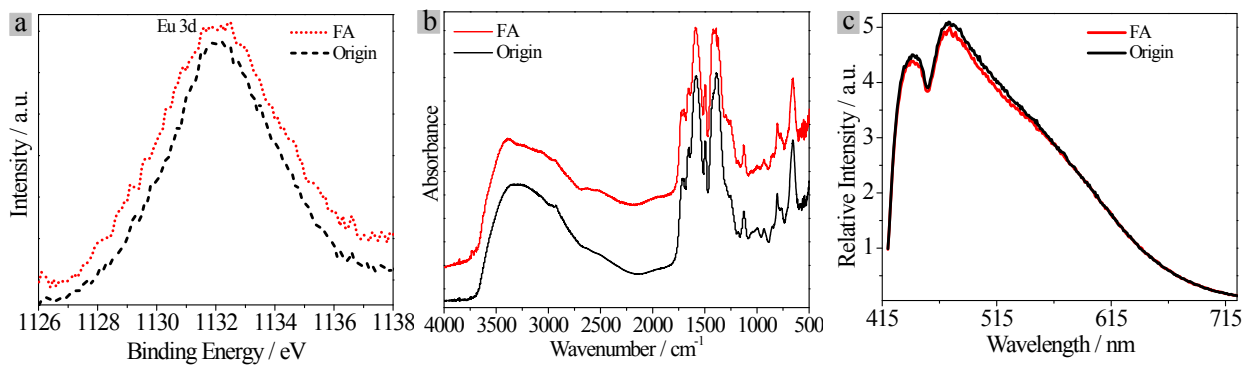


Figure S14. The Eu 3d XPS (a) and FT-IR (b) spectra for Eu^{3+} -doped **1** before and after exposure to FA; (c) The emission spectra of **1** before and after exposure to FA ($\lambda_{\text{ex}} = 375 \text{ nm}$).

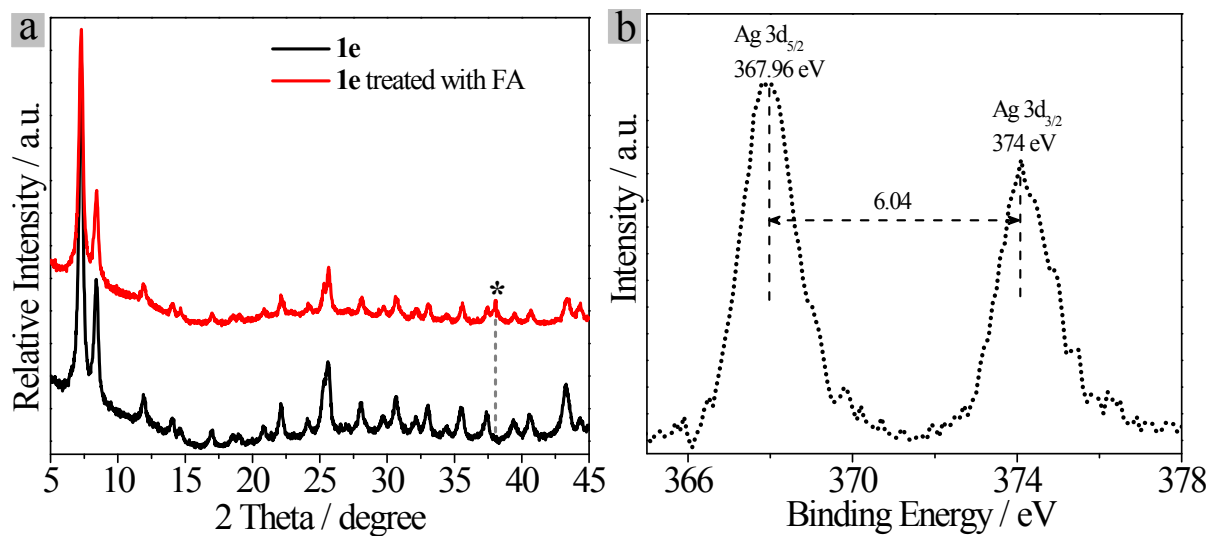


Figure S15. PXRD patterns of **1e** before and after treated by FA; (b) The Ag 3d XPS for **1e** after treatment with FA vapors.

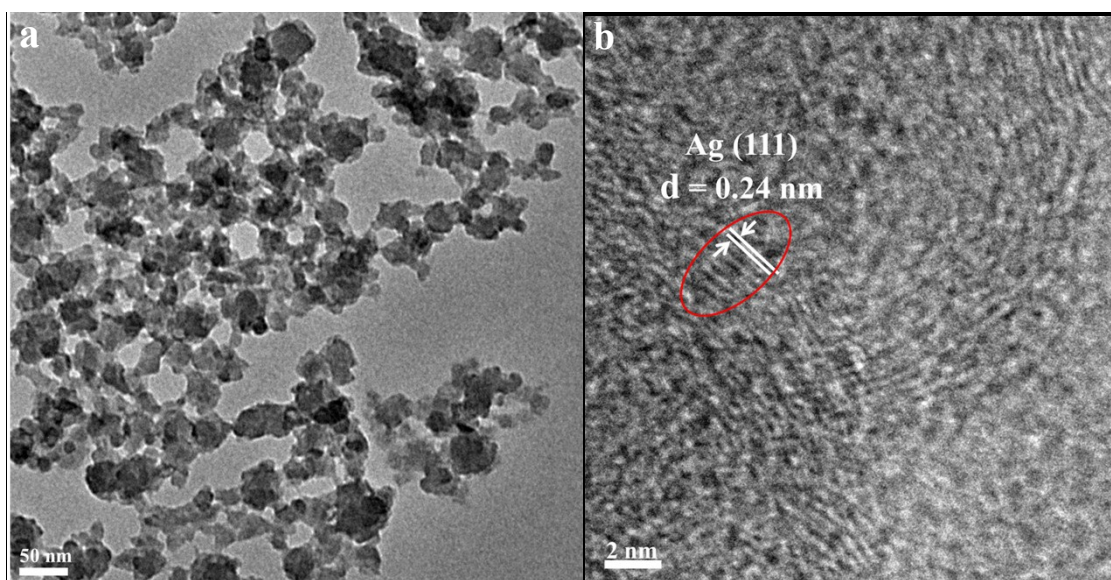


Figure S16. TEM image (a) and HR-TEM image (b) of **1e** after treated with FA.